Geochemical Perspectives Letters

Dissolved molybdenum asymptotes in sulfidic waters

G.R. Helz*

OPEN ACCESS

doi: 10.7185/geochemlet.2129

Abstract

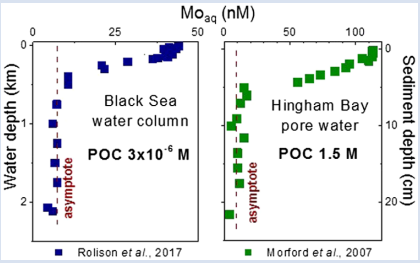

Molybdenum enrichment in organic-rich sediments is well known and is an accepted proxy for sulfidic conditions during sedimentation, but debate persists about how Mo enrichment arises. Organic scavenging and sulfide precipitation are the processes most often invoked. When dissolved Mo (Mo_{aq}) precipitates solely within sulfidic pore waters of sediments, contiguous particulate organic carbon concentrations (POC) are orders of magnitude higher than when it precipitates in euxinic water columns. Nevertheless, in both cases, Mo_{aq} concentrations decline until reaching quite similar asymptotes centred around 7.8 nM. That Mo_{aq} asymptotes are independent of organic carbon availability is inconsistent with organic scavenging as the dominant Mo fixing mechanism. In contrast, the $FeMoS_4$ precipitation mechanism predicts both the existence of asymptotes and their POC independence. Because asymptotes block quantitative Mo_{aq} precipitation, final δ^{98}Mo values in euxinic marine sediments are apt to be offset from those in seawater, but the difference is small in modern environments because $(Mo_{aq})_{asymptote} << (Mo_{aq})_{seawater}$. Asymptotes lie above the Mo_{aq} concentration believed to limit Mo nitrogenase biosynthesis, suggesting that without substantial acidification, global euxinia cannot deplete Mo_{aq} sufficiently to create marine nitrogen crises.

Received 16 December 2020 | Accepted 10 September 2021 | Published 15 October 2021

Existence and Characteristics of Asymptotes

In the oxic ocean, dissolved Mo (Mo_{aq}) is almost entirely MoO_4^{2-}. Particulate Mo (Mo_s) constitutes <0.001 % of ΣMo, except near terrigenous or hydrothermal particle sources (Ho *et al.*, 2018). However, where H_2S or HS^- replaces dissolved O_2, MoO_4^{2-} becomes thiolated, and Mo_{aq} concentrations fall sharply toward asymptotes while Mo_s in contiguous sediments rises. The resulting elevated Mo_s is interpreted as signifying sulfide's presence during sedimentation.

A compilation in Table 1 shows that the span of Mo_{aq} asymptote concentrations in diverse sulfidic environments is remarkably narrow. Entries in Table 1 meet the criteria that (a) a water column or pore water becomes sulfidic at depth, (b) Mo_{aq} drops markedly (by >50 %) below where sulfide first appears, and (c) Mo_{aq} ultimately stabilises at asymptotes (designated $Mo_{aq,\infty}$) that are distinctly above analytical detection limits. The median asymptote value is 7.8 nM, and four fifths of the values fall in the range 2.5–13.3 nM. Asymptotes are prevalent in nature, but not universal; beneath some lakes and coastal embayments, pore water Mo_{aq} concentrations fall to minima before rising at greater depths (see Morford *et al.*, 2009; Dahl *et al.*, 2010; Havig *et al.*, 2015; Sulu-Gambari *et al.*, 2017). The reason for this atypical pattern is unclear; infiltration of groundwater from surrounding uplands or very slow reductive dissolution of Mo-rich detrital phases sourced from nearby land may be contributing factors.

Of particular importance in Table 1 is the million-fold range of particulate organic carbon (POC) concentrations (expressed per unit volume of solution). For instance, during diagenesis, solutes in Hingham Bay's sulfidic pore waters are in diffusive contact with ~1.5 moles POC/L (calculated for sediments with 3.2 % total organic carbon, porosity = 0.8, and 2.5 g/cm^3 dry density; see Note II in the Supplementary Information). In contrast, measured POC concentrations in the Black Sea's sulfidic deep waters are 2.5–5.0 × 10^{-6} mol/L (Kaiser *et al.*, 2017). Despite the 10^6 difference, similar $Mo_{aq,\infty}$ asymptotes occur in both places. It could be argued that a mismatch in renewal rates of water and organic particles in the Black Sea makes this apparent POC disparity misleading. Below 1 km depth, the Black Sea's water is renewed every ~10^3 yr whereas its POC is renewed every ~10^1 yr (estimated from the POC accumulation rate in underlying sediments; Arthur *et al.*, 1994). Thus, deep water is *cumulatively* exposed to 10^2 times more POC than is present *instantaneously*. On this basis, the Black Sea's POC concentration is only 10^4, rather than 10^6, times smaller than Hingham Bay's, but the disparity is still huge.

Asymptotes are likewise insensitive to final S^{-II} concentrations (Table 1). For example, the maximum S^{-II} concentration in the Black Sea is 0.4 mM and that in Kyllaren Fjord is 5.0 mM, but both reach similar $Mo_{aq,\infty}$ asymptotes. The extreme $Mo_{aq,\infty}$ asymptotes in Table 1 (*i.e.* Walker Lake, 130 nM, and York River, 1.1 nM) mirror pH extremes, hinting that pH explains some of the asymptote variation, though the data are insufficient to establish this for certain. Any explanation for Mo_{aq} removal from sulfidic natural waters must account for why asymptotes are insensitive to ΣS^{-II} (= H_2S_{aq} + HS^-) and POC, but possibly sensitive to pH.

Departments of Geology and Chemistry, University of Maryland, College Park MD 20742, USA
* Corresponding author (email: helz@umd.edu)

Table 1 Limits to the degree of dissolved Mo removal from sulfidic environments ($Mo_{aq,0}$ = dissolved Mo at onset of sulfidic conditions; $Mo_{aq,\infty}$ = dissolved Mo at asymptote; S^{-II} is total dissolved sulfide range over depths where $Mo_{aq,\infty} \approx$ constant). For sources of data, see Note I in the Supplementary Information.

Removal within:	pH	S^{-II} (mM)	Particulate POC* (mM)	$Mo_{aq,0}$ (nM)	$Mo_{aq,\infty}$ (nM)	$Mo_{aq,\infty}/Mo_{aq,0}$ (%)
Euxinic marine water columns						
Black Sea (1991)		0.30–0.41	0.0025	36	**2.6**	7
Black Sea (2011)	7.6	0.30–0.37		37	**7.8**	21
Black Sea (2017		0.35–0.42	0.0025–0.005	41	**5.9**	14
Black Sea (2019)	7.34	0.31–0.36		36	**6.9**	19
Framvaren Fjord	7.1	0.30–7.20	0.0027 ± 0.0006	50	**17.2**	34
Kyllaren Fjord		4.23–5.02	0.003–0.008	71	**7.5**	11
Rogoznica Lake (Sept.)	7.2	0.42–2.34	0.24 ± 0.10	97	**4.5**	5
Sulfidic pore waters						
Chesapeake Bay	7.2	1.15		55	**7.8**	14
Guaymas Basin (MUC9, >25 cm)		0.12–0.43	1580 ± 68	130	**12.3**	9
Hingham Bay (Oct. 2001, >7 cm)		0.49–1.01	1530 ± 79	112	**9.3**	8
Landsort Deep (LD 1)		1.73–2.09	2200 ± 900	26	**2.1**	8
Long Island Sound (FOAM, >20 cm)		2.5–3.3	680 ± 120	115	**13.3**	12
Storfjärden (Stn 3)		0.005–0.45	2100 ± 300	30	**8.**	27
Terrebonne Bay (9A)	7.0	0.09–1.61		33	**7.3**	22
Walker Lake (WL-2)	8.4	5.4–6.2	620–1100	5700	**134.**	2
York River groundwater	6.9	0.91–1.60		73	**1.1**	2
Euxinic lake water columns						
Fayetteville Green Lake	6.9	0.44–1.86	0.066	121	**13.2**	11
Lago Cadagno (Aug 2007)	7.1	0.10	0.0068	14	**2.5**	18
Lake Fryxell	7.5	0.30–1.20	0.062 ± 0.023	26	**3.5**	13
Mahoney Lake	7.4	35.0		230	**12.**	5
Median					**7.8**	12

*Particulate POC concentrations are expressed per litre of solution. Where more than three POC measurements are available, mean ± standard deviation is reported; otherwise, the range is given.

Organic Scavenging

The principal argument for organic scavenging rests on correlations commonly, but not universally, observed between Mo_s and organic matter in sedimentary rocks. As reviewed by Helz and Vorlicek (2019), no satisfactory molecular mechanism to explain Mo_{aq} scavenging by organic matter under natural conditions has yet been found, and evidence is also lacking for significant biological scavenging. If organic scavenging exists, it is likely to be an abiotic process that can be described by a Langmuir isotherm as:

$$\frac{Mo_s}{x_s POC} = \left[\frac{K_n' x_n}{1 + K_n' x_n Mo_{aq}}\right] Mo_{aq} \qquad \text{Eq. 1}$$

where Mo_s is non-lithogenic Mo adsorbed onto particulate organic carbon (mol Mo_s/L), x_s the mole fraction of a specific binding site (mol sites/mol C), POC the particulate organic carbon concentration (mol/L), K_n' the conditional binding constant (L/mol) for the n^{th} $MoO_{4-n}S_n^{2-}$ ion, and x_n the mole fraction of the n^{th} $MoO_{4-n}S_n^{2-}$ ion in Mo_{aq} (see Fig. 1).

For simplicity, Equation 1 assumes only one adsorbing $MoO_{4-n}S_n^{2-}$ species and only one binding site. Multiple species or sites could be included by adding more terms. At the pH and Mo_{aq} concentrations of most sulfidic natural waters, the second term in the denominator is negligible, making isotherms linear. In the linear case, Equation 1 is tantamount to the empirical Mo_s/POC *vs.* Mo_{aq} relationship found for euxinic basin sediments by Algeo and Lyons (2006; see their Fig. 8a).

What does the linear form imply about aqueous asymptotes? Mass balance requires that:

$$Mo_{aq} = Mo_{aq,0} - Mo_s = Mo_{aq,0} - x_s POC[K_n' x_n] Mo_{aq} \qquad \text{Eq. 2}$$

where $Mo_{aq,0}$ is the initial total dissolved Mo and Mo_{aq} is the same during adsorption progress. Rearranging:

$$\frac{Mo_{aq}}{Mo_{aq,0}} = \frac{1}{1 + x_s POC[K_n' x_n]} \qquad \text{Eq. 3}$$

In diverse euxinic basins and sulfidic pore waters, asymptotes fix the ratio on the left hand side of this equation at a median value of 12 % (seventh column, Table 1). This requires that in nature the denominator's second term has a restricted range centred near 8. Given the 10^6 range of its POC factor, this requirement cannot possibly be met. Additionally, at any specific site, the ratio on the left is roughly constant through the asymptote zone, requiring that the second term in the denominator is also constant. However, H_2S_{aq} varies through asymptote zones (third column, Table 1), and x_n values strongly vary with H_2S_{aq} (Fig. 1). Only at high H_2S_{aq} concentrations, where x_4 becomes sulfide independent, can Equation 3 describe constant asymptotes at a constant POC concentration. (In this case, x_4 replaces x_n in Equation 3, implying that MoS_4^{2-} is the only adsorbed

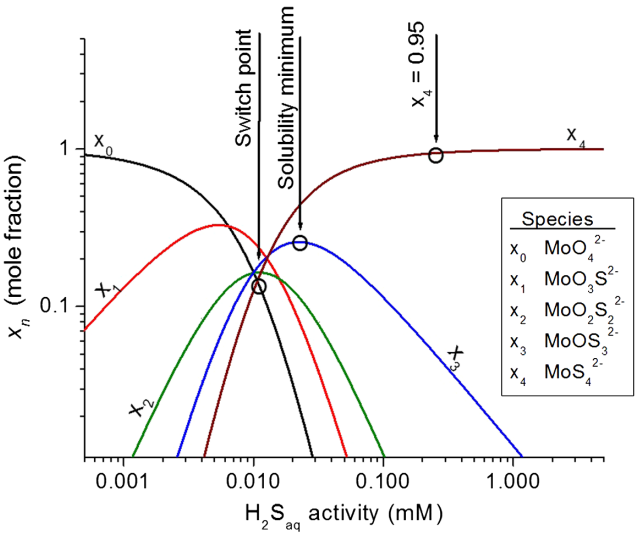

Figure 1 Mole fractions of aqueous $MoO_{4-n}S_n^{2-}$ species *versus* the activity of H_2S_{aq}, which is the non-ionised fraction of total dissolved sulfide. Circles mark three special points: where $MoO_4^{2-} = MoS_4^{2-}$ (switch point); where x_3 reaches its maximum (corresponding to the solubility minimum); and where $x_4 \geq 0.95$, signifying effective completion of Mo_{aq} thiolation.

species.) However, H_2S_{aq} concentrations high enough for x_4 to approach constancy exceed the concentrations at which Mo_{aq} asymptotes commence in nature. For example, the Mo_{aq} asymptote in the Black Sea commences at $H_2S_{aq} \approx 50$ μM (where $\Sigma S^{-II} \approx 300$ μM), whereas Figure 1 shows that H_2S_{aq} must be much higher, near 200 μM, for x_4 to come within 5 % of its ultimate limiting value. Equation 3, which describes organic scavenging, therefore cannot explain Mo_{aq} asymptotes.

$FeMoS_4$ Precipitation

Earlier workers rejected the possibility of Mo precipitation by sulfide. Emerson and Huested (1991) pointed out that, unlike sulfide-precipitated metals, Mo_{aq} fails to decline continuously with increasing ΣS^{-II}. In agreement, Algeo and Lyons (2006) noted that Cariaco Basin sediments accumulate higher Mo_s concentrations than Black Sea sediments, even though Cariaco waters contain less sulfide.

Nevertheless, Vorlicek *et al.* (2018) found a colloidal precipitate, $FeMoS_4$, with a solubility that could explain Mo_{aq} asymptotes in the Black Sea. At equilibrium with this precipitate (see derivation in Note III, Supplementary Information):

$$Mo_{aq} = \frac{10^{-19.83}10^{2pH}}{Q_{FeS}(\gamma_{MoS_4})}(x_3)^{-1} \qquad \text{Eq. 4}$$

where γ_{MoS_4} is the activity coefficient of MoS_4^{2-} and $Q_{FeS} = \{Fe^{2+}\}\{H_2S_{aq}\}/\{H^+\}^2$. Except for the x_3 term, the factors on the righthand side of Equation 4 display limited variability in asymptote zones. Q_{FeS} values are usually constrained by saturation with iron monosulfide phases and pH is constrained mainly by strong $\Sigma CO_2/\Sigma ALK$ buffering. On the other hand, x_3 varies considerably, passing through a maximum with increasing H_2S_{aq} activity (Fig. 1). In Table 2, values of H_2S_{aq} at x_3 maxima have been estimated over a moderate temperature range by the isocoulombic extrapolation method (Gu *et al.*, 1994). Equation 4 requires that at x_3 maxima, Mo_{aq} solubility reaches minima; this is illustrated by dashed curves in Figure 2. However, aging transforms $FeMo^{VI}S_4$ to an inert Mo^{IV} phase, preventing Mo redissolution when the solubility curves turn upward beyond the minima. As a result, the $FeMoS_4$ precipitation mechanism predicts that Mo_{aq} becomes fixed at asymptotes that are unresponsive to further H_2S_{aq} increases. The asymptotes are also independent of POC, despite the 10^6 range in nature, because organic matter has no role in the precipitation and aging reactions, except as fuel for biological sulfate reduction (Helz and Vorlicek, 2019). Thus $FeMoS_4$ precipitation meets the requirements listed above for a mechanism that can explain asymptotes.

Table 2 Concentrations of H_2S_{aq} (μM) at selected temperatures and degrees of MoO_4^{2-} thiolation (ionic strength = 0).

Temperature (°C)	Switch point ($MoO_4^{2-} = MoS_4^{2-}$)	Solubility minimum ($MoOS_3^{2-}$ peak)	$x_4 = 0.95$ (thiolation ≈ complete)
5	5	9	120
25	11	21	260
45	22	42	530

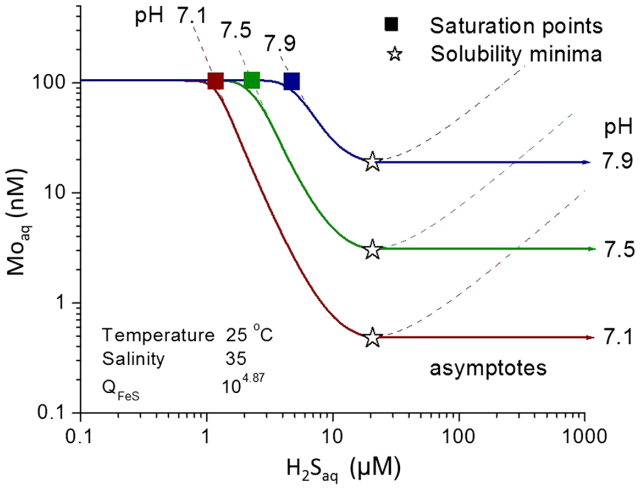

Figure 2 Effect of rising H_2S_{aq} on $FeMoS_4$ solubility (dashed curves) in seawater (initial $Mo_{aq} = 105$ nM) assuming saturation with FeS_{nano}, a material more soluble and reactive than mackinawite (Wolthers *et al.*, 2005; Matamoros-Veloza *et al.*, 2018). At $FeMoS_4$ saturation points (squares), the solubility drops below ambient $Mo_{aq,0}$ and precipitation begins. Eventually, solubility minima (stars) are reached. Actual Mo_{aq} follows the heavy curves because an irreversible redox transformation blocks redissolution of precipitated Mo. Based on Equation 2 in Helz and Vorlicek (2019).

Implications

Several implications of interest in the palaeoproxy field arise from this result.

Asymptotes block quantitative removal of Mo_{aq} from sulfidic waters, leaving dissolved residuals that ultimately escape the sulfidic environment. In the median case in Table 1, the residual ($Mo_{aq,\infty}/Mo_{aq,0}$) is only 12 % but can be much higher. This finding undermines the common assumption that marine euxinic basins preserve the $\delta^{98}Mo$ signatures of global seawater because of quantitative precipitation. Residuals will be greatest in waters of lower salinity, where $Mo_{aq,0}$ will be lower, and in

waters of higher pH, where $Mo_{aq,\infty}$ will be higher. Both situations generate higher $Mo_{aq,\infty}/Mo_{aq,0}$ ratios at asymptotes, permitting larger fractions of incoming Mo_{aq} to escape deposition.

The idea that Mo_s/POC ratios in sedimentary rocks can be used to estimate Mo_{aq} in ancient basins (Algeo and Lyons, 2006, and others) relies on the relationship in Equation 1, which is premised on the dominance of POC scavenging. Without scavenging, such Mo_{aq} estimates are ungrounded.

Table 1 shows that Mo_{aq} asymptotes in the pH range of modern environments all exceed 1 nM, the level thought to curb nitrogen fixation by Mo-nitrogenase (Glass *et al.*, 2010). Therefore, past global euxinia would not have shut down Mo-nitrogenase activity, creating marine nitrogen crises, unless accompanied by substantial acidification, which lowers $Mo_{aq,\infty}$ (Fig. 2).

Can $FeMoS_4$ precipitation explain why the Black Sea produces lower sedimentary Mo_s despite higher bottom water H_2S_{aq} concentrations compared to the Cariaco Basin? Consistent with the organic scavenging mechanism (Eq. 1), Algeo and Lyons (2006) regarded bottom water Mo_{aq} concentration, which is lower in the Black Sea, as the controlling variable. The Black Sea's lower bottom water Mo_{aq} concentration, and consequent lower sediment Mo_s concentration, were attributed to a Mo_{aq} supply restriction at the narrow Bosporus. This explanation is probably incorrect. The Bosporus distributes 4–5 times more Mo_{aq} into the Black Sea than its sediments accumulate (Piper and Calvert, 2009), and the excess returns through the Bosporus. On the other hand, the Bosporus restricts the Black Sea's river water throughput. Copious river inflow lowers surface salinity and intensifies density stratification, thus inhibiting introduction of oxidants into deep waters. Consequently, ΣS^{-II} accumulates sufficiently for the $FeMoS_4$ saturation point to ascend into the water column, causing Mo_{aq} drawdown there. Cariaco's better ventilation, attested by its shorter water residence time, suppresses ΣS^{-II} despite opposition from a greater POC rain rate. This confines Cariaco's saturation point to pore waters. Calculations based on ΣS^{-II} and pH data suggest that the Black Sea's saturation point is near 150 m depth in the water column, whereas Cariaco's is located a few mm below the sediment–water interface (Helz and Vorlicek, 2019). Therefore, Cariaco's bottom waters are pre-asymptote, whereas the Black Sea's are syn-asymptote. Cariaco's sediments accumulate more Mo_s by diffusion because of the very sharp, pre- to syn-asymptote Mo_{aq} gradient across the sediment–water interface.

To summarise, the narrow range of $Mo_{aq,\infty}$ values that form in sulfidic water columns and pore waters characterised by enormous differences in POC concentrations preclude adsorption to organic matter as an important Mo fixation process in nature. In contrast, $FeMoS_4$ precipitation, which depends on the thermodynamic activities of H^+, MoS_4^{2-}, and FeS rather than their concentrations, readily explains why Mo_{aq} asymptotes are independent of final sulfide and POC concentrations.

Editor: Liane G. Benning

Additional Information

Supplementary Information accompanies this letter at https://www.geochemicalperspectivesletters.org/article2129.

Cite this letter as: Helz, G.R. (2021) Dissolved molybdenum asymptotes in sulfidic waters. *Geochem. Persp. Let.* 19, 23–26.

References

Algeo, T.J., Lyons, T.W. (2006) Mo-total organic carbon covariation in modern marine environments: Implication for analysis of paleoredox and paleohydrographic conditions. *Paleooceanography and Paleoclimatology* 21, PA1016.

Arthur, M.A., Dean, W.E., Neff, E.D., Hay, B.J., King, J., Jones, G. (1994) Varve calibrated records of carbonate and organic carbon accumulation over the last 2000 years in the Black Sea. *Global Biogeochemical Cycles* 8, 195–217.

Dahl, T.W., Anbar, A.D., Gordon, G.W., Rosing, M.T., Frei, R., Canfield, D.E. (2010) The behavior of molybdenum and its isotopes across the chemocline and in the sediments of sulfidic Lake Cadagno, Switzerland. *Geochimica et Cosmochimica Acta* 74, 144–163.

Emerson, S.R., Huested, S.S. (1991) Ocean anoxia and the concentrations of molybdenum and vanadium in seawater. *Marine Chemistry* 34, 177–196.

Glass, J.B., Wolfe-Simon, F., Elser, J.J., Anbar, A.D. (2010) Molybdenum-nitrogen co-limitation in freshwater and coastal heterocystous cyanobacteria. *Limnology and Oceanography* 55, 667–676.

Gu, Y., Gammons, C.H., Bloom, M.S. (1994) A one-term extrapolation method for estimating equilibrium constants of aqueous reactions at elevated temperatures. *Geochimica et Cosmochimica Acta* 58, 3545–3560.

Havig, J.R., McCormick, M.L., Hamilton, T.L., Kump, L.R. (2015) The behavior of biologically important trace elements across the oxic/euxinic transition of meromictic Fayettville Green Lake, New York, USA. *Geochimica et Cosmochimica Acta* 165, 389–406.

Helz, G.R., Vorlicek, T.P. (2019) Precipitation of molybdenum from euxinic waters and the role of organic matter. *Chemical Geology* 509, 178–193.

Ho, P., Lee, J.-M., Heller, M.I., Lam, P.J., Shiller, A.M. (2018) The distributions of dissolved and particulate Mo and V along the U.S. GEOTRACES East Pacific zonal transect (GP16): The roles of oxides and biogenic particles in their distribution in the oxygen deficient zone and the hydrothermal plume. *Marine Chemistry* 201, 242–255.

Kaiser, D., Konovalov, S., Schulz-Bull, D.E., Waniek, J.J. (2017) Organic matter along longitudinal and vertical gradients in the Black Sea. *Deep Sea Research Part I* 129, 22–31.

Matamoros-Veloza, A., Cespedes, O., Johnson, B.R.G., Stawski, T.M., Terranova, U., de Leeuw, N.H., Benning, L.G. (2018) A highly reactive precursor in the iron sulfide system. *Nature Communications* 9, 3125.

Morford, J.L., Martin, W.R., Kalnejais, L.H., François, R., Bopthner, M., Karle, I.-M. (2007) Insights on geochemical cycling of U, Re and Mo from seasonal sampling in Boston Harbor, Massachusetts, USA. *Geochimica et Cosmochimica Acta* 71, 895–915.

Morford, J.L., Martin, W.R., François, R., Carney, C.M. (2009) A model for uranium, rhenium and molybdenum diagenesis in marine sediments based on results from coastal locations. *Geochimica et Cosmochimica Acta* 73, 2938–2960.

Piper, D.Z., Calvert, S.E. (2009 A marine biogeochemical perspective on black shale deposition. *Earth-Science Reviews* 95, 63–96.

Rolison, J.M., Stirling, C.H., Middag, R., Rijkenberg, M.J.A. (2017) Uranium stable isotope fractionation in the Black Sea: Modern calibration of the $^{238}U/^{235}U$ paleo-redox proxy. *Geochimica et Cosmochimica Acta* 203, 69–88.

Sulu-Gambari, R., Roepert, A., Jilbert, T., Hagens, M., Meysman, F.J.R., Slomp, C.P. (2017) Molybdenum dynamics in sediments of a seasonally-hypoxic coastal marine basin. *Chemical Geology* 466, 627–640.

Vorlicek, T.P., Helz, G.R., Chappaz, A., Vue, P., Vezina, A., Hunter, W. (2018) Molybdenum burial mechanism in sulfidic sediments: iron-sulfide pathway. *ACS Earth and Space Chemistry* 2, 565–576.

Wolthers, M., Charlet, L., van der Linde, P.R., Rickard, D., van der Weijden, C.H. (2005) Surface chemistry of disordered mackinawite (FeS). *Geochimica et Cosmochimica Acta* 69, 3469–3481.

Geochemical Perspectives Letters

Dissolved molybdenum asymptotes in sulfidic waters

G.R. Helz

Supplementary Information

The Supplementary Information includes:

- Sources for Data Compiled in Table 1
- Note on Calculation of POC Values for Pore Waters in Table 1
- Derivation of Equation 4
- Supplementary Information References

Sources of Data Compiled in Table 1

Location	Reference
Euxinic marine waters	
Black Sea (1991)	Emerson, S.R., Huested, S.S. (1991) Ocean anoxia and the concentrations of molybdenum and vanadium in seawater. *Marine Chemistry* 34, 177–196.
	Karl, D.M., Knauer, G.M. (1991) Microbial production and particle flux in the upper 350 m of the Black Sea. *Deep-Sea Research* 38(Supple 2), S921–S942.
Black Sea (2011)	Nägler, T.F., Neubert, N., Böttcher, M.E., Dellwig, O., Schnetger, B. (2011) Molybdenum isotope fractionation in pelagic euxinia: Evidence from the modern Black and Baltic Seas. *Chemical Geology* 289, 1–11.
Black Sea (2017)	Rolison, J.M., Stirling, C.H., Middag, R., Rijkenberg, M.J.A. (2017) Uranium stable isotope fractionation in the Black Sea: Modern calibration of the $^{238}U/^{235}U$ paleo-redox proxy. *Geochimica et Comochimica Acta* 203, 69–88.
	Kaiser, D., Konoalov, S., Schulz-Bull, D.E., Waniek, J.J. (2017) Organic matter along longitudinal and vertical gradients in the Black Sea. *Deep-Sea Research I* 129, 22–31.
Black Sea (2019)	Dellwig, O., Wegwerth, A., Schnetger, B., Schulz, H., Arz, H.W. (2019) Dissimilar behaviors of the geochemical twins W and Mo in hypoxic-euxinic marine basins. *Earth-Science Reviews* 193, 1–23.

	Hiscock, W.T., Millero, F.J. (2006) Alkalinity of the anoxic wars in the Western Black Sea. *Deep-Sea Research II* 53, 1787–1801.
Framvaren Fjord	Emerson, S.R., Huested, S.S. (1991) Ocean anoxia and the concentrations of molybdenum and vanadium in seawater. *Marine Chemistry* 34, 177–196.
	Landing, W.M., Westerlund, S. (1988) The solution chemistry of iron(II) in Framvaren Fjord. *Marine Chemistry* 23, 329–343.
	Velinsky, D.J., Fogel, M.L. (1999) Cycling of dissolved and particulate nitrogen and carbon in the Framvaren Fjord, Norway: stable isotopic variations. *Marine Chemistry* 67, 161–180.
Kyllaren Fjord	Noordmann, J., Weyer, S., Montoya-Pino, C., Dellwig, O., Neubert, N., Eckert, S., Paetzel, M., Böttcher, M.E. (2015) Uranium and molybdenum isotope systematics in modern euxinic basins: Case studies from the central Baltic Sea and Kyllaren Fjord (Norway). *Chemical Geology* 396, 182–195.
Rogoznica Lake (Sept.)	Helz, G.R., Bura-Nakić, E., Mikac, N., Ciglenečki, I. (2011) New model for molybdenum behavior in euxinic waters. *Chemical Geology* 284, 323–332.
	Čanković, M., Žučko, J., Radić, D., Janeković, I., Petrić, I., Ciglenečki, I., Collins, G. (2019) Microbial diversity and long-term geochemical trends in the euxinic zone of a marine, meromictic lake. *Systematic and Applied Microbiology* 42, 126016.
Sulfidic pore waters	
Chesapeake Bay (2021)	Cui, M., Luther, G.W. III, Gomes, M. (2021) Cycling of W and Mo species in natural sulfidic waters and their sorption mechanism on MnO_2 and implications for paired W and Mo records as a redox proxy. *Geochimica et Comochimica Acta* 295, 24–48.
Guaymas Basin (MUC9)	Eroglu, S, Scholz, F., Siebert, C. (2020) Influence of particulate versus diffusive molybdenum supply mechanisms on the molybdenum isotope composition of continental margin sediments. *Geochimica et Comochimica Acta* 273, 51–69.
Hingham Bay (Oct. 2001)	Morford, J.L., Martin, W.R., Kalnejais, L.G., François, R., Bothner, M., Karle, I.-M. (2007) Insights on geochemical cycling of U, Re and Mo from seasonal sampling in Boston Harbor, Massachusetts, USA. *Geochimica et Comochimica Acta* 71, 895–915.
	Kalnejais, L.H., Martin, W.R., Bothner, M.H. (2015) Porewater dynamics of silver, lead and copper in coastal sediments and implications for benthic metal fluxes. *Science of the Total Environment* 517, 178–194.
Landsort Deep (LD 1)	Dellwig, O., Wegwerth, A., Schnetger, B., Schulz, H., Arz, H.W. (2019) Dissimilar behaviors of the geochemical twins W and Mo in hypoxic-euxinic marine basins. *Earth-Science Reviews* 193, 1–23.
Long Island Sound (FOAM)	Hardisty, D.S., Lyons, T.W., Riedinger, N., Isson,T.T., Owens, J.D., Aller, R.C., Rye, D.M., Planavsky, N.J., Reinhard, C.T., Gill, B.C., Masterson, D.A., Johnston, D.T. (2018) An evaluation of sedimentary molybdenum and iron as proxies for pore fluid paleoredox conditions. *American Journal of Science* 318, 527–556.
Storfjärden (Stn 3) Northern Baltic	Jokinen, S.A., Koho, K., Virtasalo, J.J., Jilbert, T. (2020) Depth and intensity of the sulfate-methane transition zone control sedimentary molybdenum and uranium sequestration in a eutrophic low salinity setting. *Applied Geochemistry* 122, 104767
Terrebonne Bay (9A)	Mohajerin, T.J., Helz, G.R., Johannesson, K.H. (2016) Tungsten-molybdenum fractionation in estuarine environments. *Geochimica et Comochimica Acta* 177, 105–119.

Walker Lake (WL-2)	Domagulski, J.L., Eugster, H.P., Jones, B.F. (1990) Trace metal geochemistry of Walker, Mono, and Great Salt Lakes. In: Spencer, R.J, Chou I.-M. (Eds.) *Fluid-Mineral Interactions: A Tribute to H.P. Eugster*. The Geochemical Society, Washington D.C., Special Publication No. 2, 315–353.
York River, Virginia	O'Connor, A.E., Luek, J.L., McIntosh, H., Beck, A.J. (2015) Geochemistry of redox sensitive trace elements in a shallow subterranean estuary. *Marine Chemistry* 172, 70–81.
Euxinic lakes	
Fayetteville Green Lake	Havig, J.R., McCormick, M.L., Hamilton, T.L., Kump, L.R. (2015) The behavior of biologically important trace elements across the oxic/euxinic transition of meromictic Fayettville Green Lake, New York, USA. *Geochimica et Comochimica Acta* 165, 389–406. Torgersen, T., Hammond, D.E., Clarke, W.B., Peng, T.-H. (1981) Fayetteville, Green Lake, New York: ^{3}H-^{3}He water mass ages and secondary chemical structure. *Limnology and Oceanography* 26, 110–122.
Lago Cadagno (Aug 2007)	Dahl, T.W., Anbar, A.D., Gordon, G.W., Rosing, M.T., Frei, R., Canfield, D.E. (2010) The behavior of molybdenum and its isotopes across the chemocline and in the sediments of sulfidic Lake Cadagno, Switzerland. *Geochimica et Comochimica Acta* 74, 144–163. Posth, N.R., Bristow, L.A., Cox, R.P., Habicht, K.S., Danza, F., Tonolla, M., Frigaard, N.-U., Canfield, D.E. (2017) Carbon isotope fractionation by anoxygenic phototrophic bacteria in euxinic like Cadagno. *Geobiology* 15, 798–816.
Lake Fryxell	Yang, N., Welch, K.A., Mohajerin, T.J., Telfeyan, K., Chevis, D.A, Grimm, D.A., Lyons, W.B., White, C.D., Johannesson, K.H. (2015) Comparison of arsenic and molybdenum geochemistry in meromictic lakes of the McMurdo Dry Valleys, Antarctica: Implications for oxyanion-forming trace element behavior in permanently stratified lakes. *Chemical Geology* 404, 110–125. Priscu, J. (2021) Particulate organic carbon (POC) and nitrogen (PON) concentrations in discrete water column samples collected from lakes in the McMurdo Dry Valleys, Antarctica (1993–2019, ongoing) ver 17. *Environmental Data Initiative*. https://doi.org/10.6073/pasta/ab14e3003e6180c6200abd6bc72441a3 (Accessed 13 July 2021).
Mahoney Lake	Reinhard, C.T. (2008) *Controls on authigenic sequestration of molybdenum in the sediments of meromictic Mahoney Lake, British Columbia*. M.S. Thesis, University of California, Riverside. 91 pp.

Note on Calculation of POC Values for Pore Waters in Table 1

It is assumed that pore waters are in diffusive contact with all the organic carbon in sediments on the time scale of diagenesis. Therefore, POC aqueous concentrations (moles C/L) can be calculated from a sediment's dry TOC concentration, sediment porosity (θ) and solid phase density (ρ) values: POC = $[C_{org}/12.0][(1-\theta)\rho/\theta]$, where C_{org} has units of g C/g dry sediment and 12.0 is the atomic mass of carbon. In a single core, θ and ρ both will vary, but their ranges are not great. For calculations in Table 1, generic and constant values for porosity (0.8) and solid phase density

(2.3 g/cm^3) were used. In nature, these values will differ from the generic values by as much as 15 %, but the error in POC arising from this simplification is negligible relative to the immense range in POC concentrations in the Table.

Derivation of Equation 4

Precipitation of $FeMoS_4$ occurs by the following reaction (Vorlicek et al. 2018):

$$Fe^{2+} + MoS_4^{2-} = FeMoS_4(s) \qquad K = \frac{1}{\{Fe^{2+}\}\{MoS_4^{2-}\}} \qquad \text{Eq. S-1}$$

(Braces designate thermodynamic activities.) $\{MoS_4^{2-}\}$ is related to Mo_{aq}, the total dissolved Mo concentration, by:

$$\{MoS_4^{2-}\} = (\gamma_{MoS4})x_4 Mo_{aq} \qquad \text{Eq. S-2}$$

Where γ_{MoS4} is the activity coefficient of the tetrathiomolybdate ion and x_4 is its mol fraction in Mo_{aq} (values plotted in Fig. 1).

Thiolation of $MoOS_3^{2-}$ to form MoS_4^{2-} occurs by (Erickson and Helz, 2000):

$$H_2S + MoOS_3^{2-} = MoS_4^{2-} + H_2O, \qquad 10^{4.88} = \frac{\{MoS_4^{2-}\}}{\{MoOS_3^{2-}\}\{H_2S\}} = \frac{x_4}{x_3\{H_2S\}} \qquad \text{Eq. S-3}$$

At the very earliest stages of biological sulfate reduction in anoxic aquatic environments, before Mo_{aq} precipitation begins, $\{Fe^{2+}\}$ becomes linked to pH and $\{H_2S_{aq}\}$, the non-ionized form of dissolved sulfide, by the solubility product constant of an iron monosulfide phase (K_{FeS}):

$$\{Fe^{2+}\} = \frac{K_{FeS}(10^{-2pH})}{\{H_2S\}} \qquad \text{Eq. S-4}$$

Substituting Equations S-2 to S-4 into S-1 yields:

$$Mo_{aq} = \frac{10^{-19.83}(10^{2pH})}{K_{FeS}(\gamma_{MoS4})} x_3^{-1} \qquad \text{Eq. S-5}$$

By replacing x_4 with x_3, the explicit $\{H_2S\}$ term has been eliminated. In this form, Equation S-5 demonstrates that under conditions of relatively constant pH and ionic strength, rising sulfide concentrations produce a solubility minimum where x_3 reaches a maximum.

Because $FeMoS_4$ precipitation is likely to occur in microniche hotspots where FeS nucleation and growth are active, Ostwald's Rule suggests that the relevant value of K_{FeS} is likely to be that of a metastable phase, such as FeS_{nano} or FeS_{Amorph}, rather than that of mackinawite. In Figure 2 in the main text, Wolthers' (2005) value of $K_{FeS} = 10^{4.87}$ is assumed.

Supplementary Information References

Erickson, B.E., Helz, G.R. (2000) Molybdenum(VI) speciation in sulfidic waters: Stability and lability of thiomolybdates. *Geochimica et Comochimica Acta* 64, 1149–1158.

Vorlicek, T.P., Helz, G.R., Chappaz, A., Vue, P., Vezina, A., Hunter, W. (2018) Molybdenum burial mechanism in sulfidic sediments: iron-sulfide pathway. *ACS Earth and Space Chemistry* 2, 565–576.

Wolthers, M., Charlet, L., van der Linde, P.R., Rickard, D., van der Weijden, C.H. (2005) Surface chemistry of disordered mackinawite (FeS). *Geochimica et Comochimica Acta* 69, 3469–3481.